

Electrodeposited zinc oxide nanorods ALD-coated with iron oxide

Photocatalytic and photoelectrochemical properties

Taha Ahmed, Mattis Fondell, Mats Boman, Jiefang Zhu

Department of chemistry–Ångström



UPPSALA
UNIVERSITET

Oct 29, 2013

Combining two semiconductors to make one photoanode

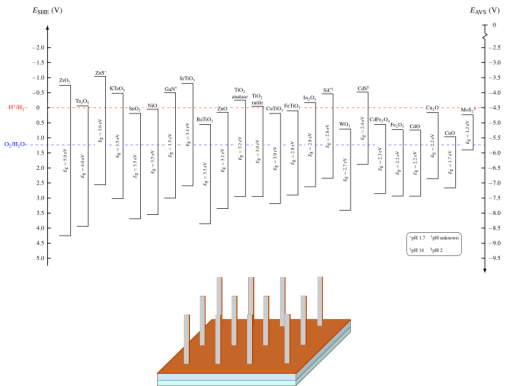
Combining two semiconductors...

to absorb more light and more colours,
to better separate photoexcited electron-hole pairs

... ZnO nanorods coated with varying thickness of iron oxide

nanorods cause increased surface area,
ZnO is white, iron oxide commonly red,
band edges fairly well matched

Tailoring morphology and electronic band structure



Electrodeposition of zinc oxide, ALD of iron oxide

Electrodeposition

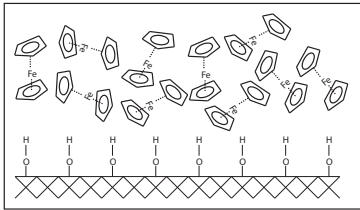
Potentiostatic cathodic deposition for 1.5 h in $\text{ZnCl}_2(\text{aq})$,
three-electrode cell, Ag/AgCl RE, Pt-wire CE

Atomic-layer deposition

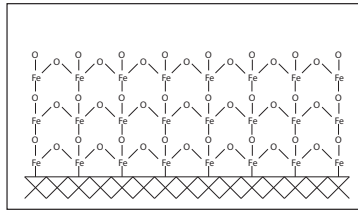
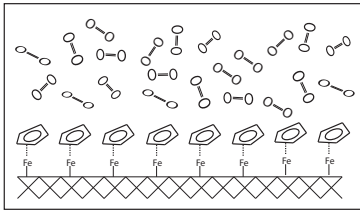
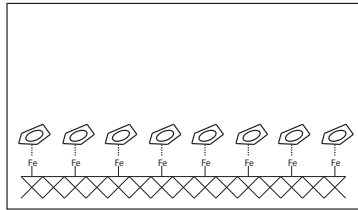
Cycles of ferrocene and oxygen gas, using Picosun ALD reactor at
 450°C ,
conditions targeted for hematite formation,
Number of cycles varied between 35 to 100 ($< 25 \text{ nm}$)

Atomic-layer deposition mechanism

Reactive cycle



Inert cycle

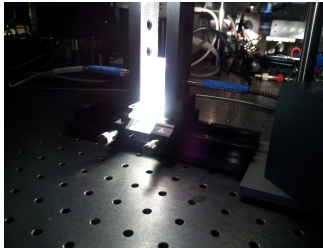
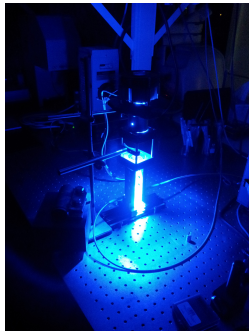


In-situ tracking of dye degradation

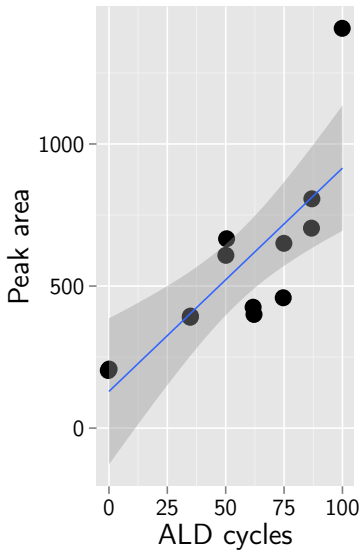
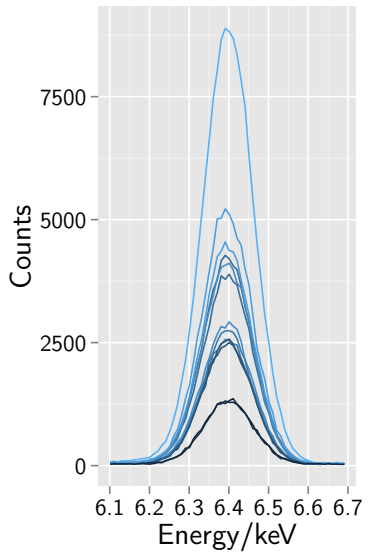
Degradation of azo dye in aqueous soln. under visible-light

Dye: eriochrome black T, 5 mg l^{-1} .

Light source: 50 W 450 nm LED.

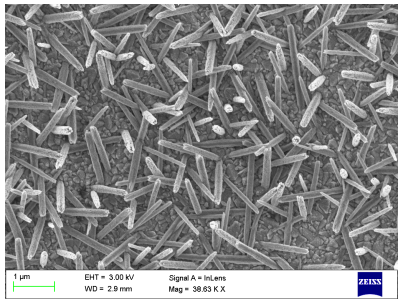


XRF: Fe KL_3 transition increases with ALD cycles

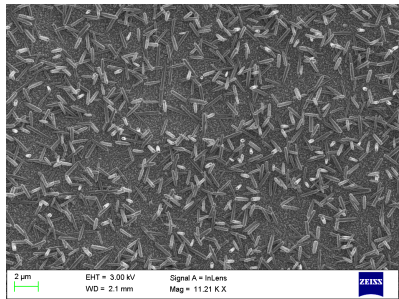


Iron-phase is so thin that it does not affect morphology

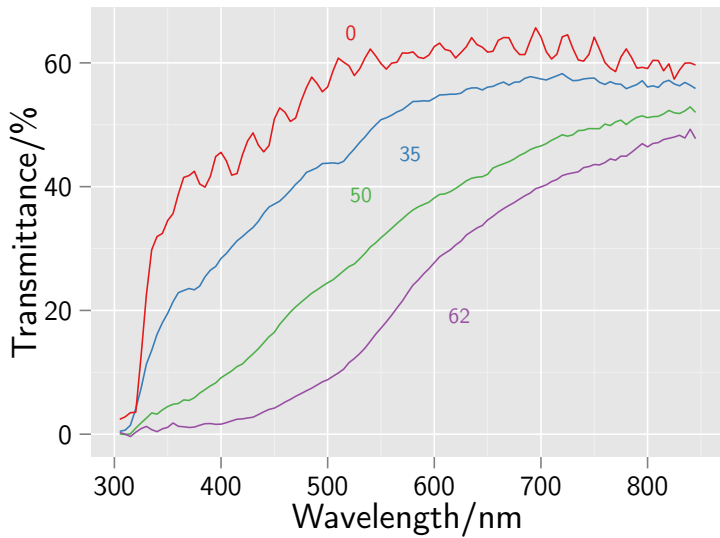
Before



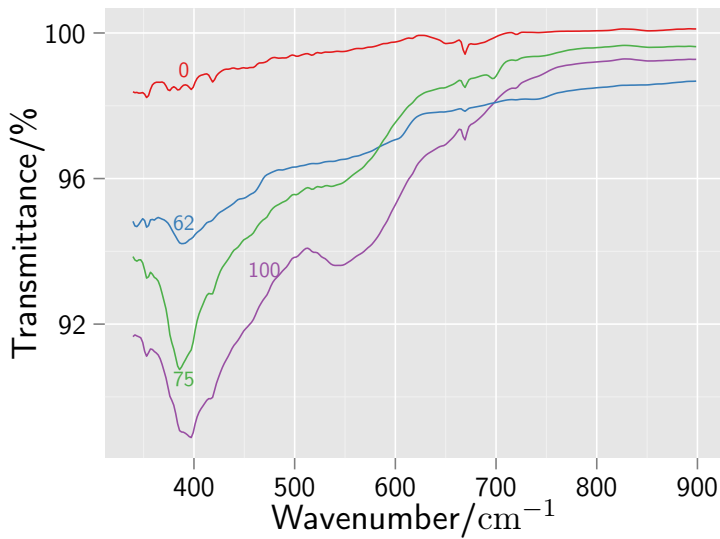
After



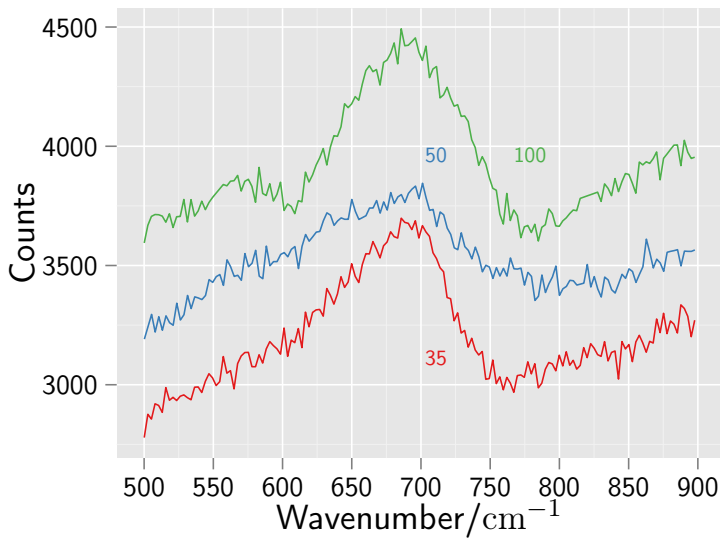
Optical spectroscopy: overall absorption increases



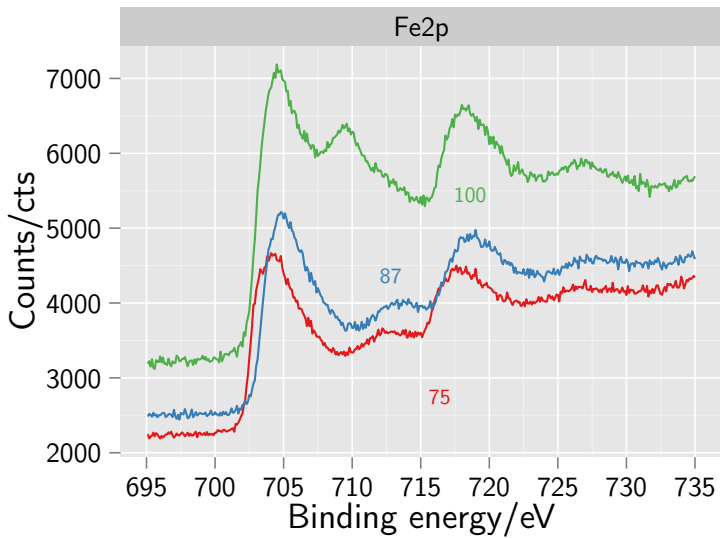
ATR-FTIR spectroscopy: hard-to-interpret weak signal



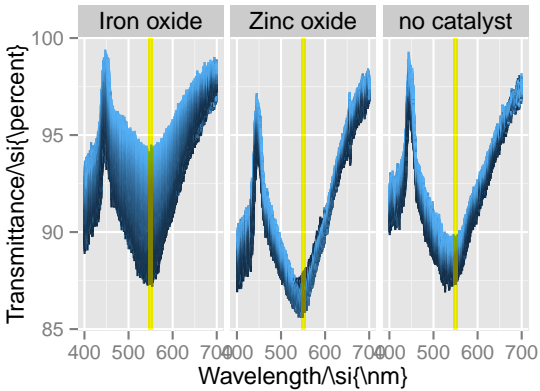
Raman spectroscopy: perhaps not pure hematite . . .



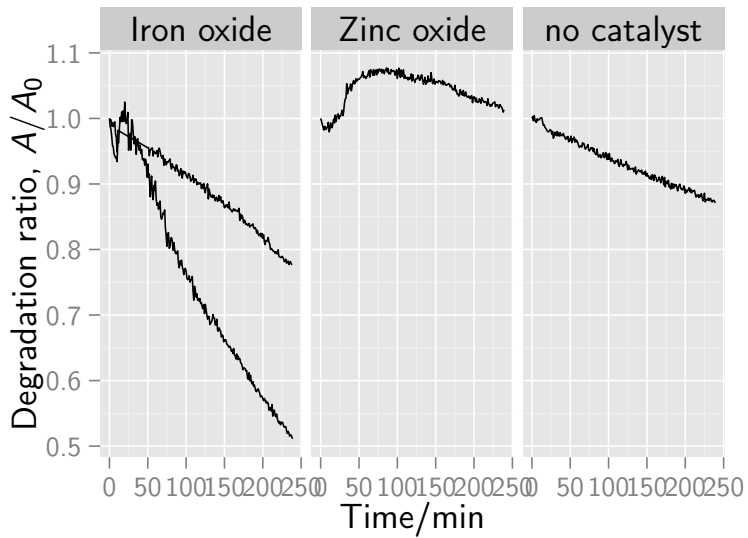
XPS: ... hematite after all?



Photocatalytic effect improves with thickness



Photocatalytic effect improves with thickness



Conclusions

Photocatalytic activity improves with increasing thickness

but even our 'thickest' coating is really thin. Perhaps the biggest gain is that the samples show very good stability under irradiation. This is due to the iron oxide coating.

Iron oxide phase

XPS strongly indicates hematite,
but poor crystallinity and very thin iron oxide layer complicates analysis.

Conclusions

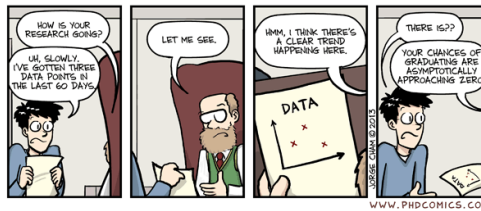
Simple preparation gives 3D-nanostructure

Addition of ultrathin conformal iron oxide layer improves stability greatly, and makes the photoanode active in visible light.

Low PC activity thought to be partly due

to small amount of visible-light-active catalyst on each sample.

Trending



Electrodeposition

Electrodeposition of zinc oxide

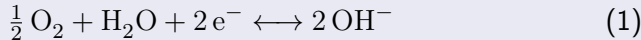


Dissolved oxygen in the electrolyte is reduced to hydroxide ions, local pH increase at the electrode's surface precipitates zinc hydroxide, zinc oxyhydroxide, and zinc oxide (temperature dependent).

Other oxygen-sources have been used, e.g., nitrate ions in solution, water. Bubbling oxygen allows easy control of O_2 concentration, and leaves no by-products.

Electrodeposition

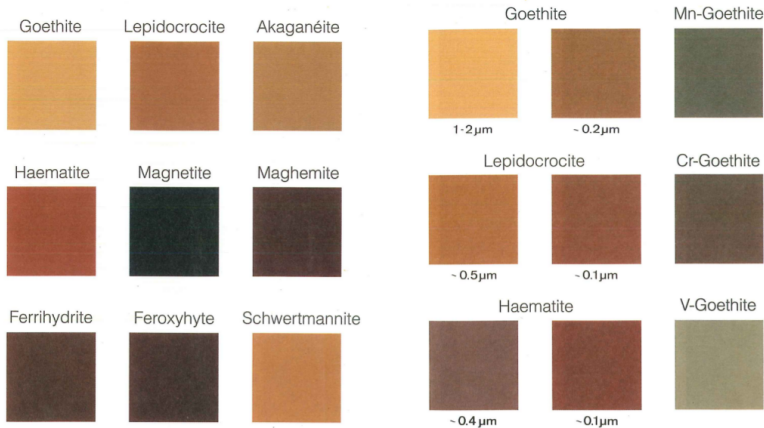
Electrodeposition of zinc oxide



Dissolved oxygen in the electrolyte is reduced to hydroxide ions, local pH increase at the electrode's surface precipitates zinc hydroxide, zinc oxyhydroxide, and zinc oxide (temperature dependent).

Other oxygen-sources have been used, e.g., nitrate ions in solution, water. Bubbling oxygen allows easy control of O_2 concentration, and leaves no by-products.

Iron oxide comes in a variety of structures and compositions

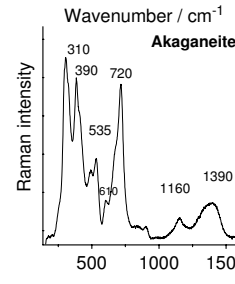
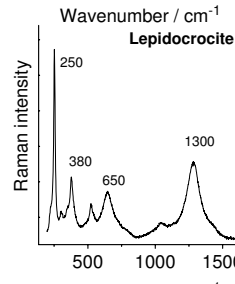
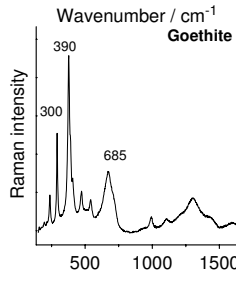
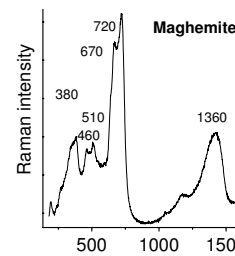
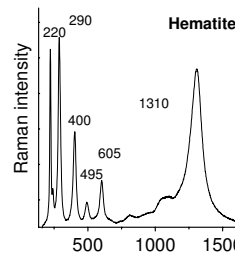
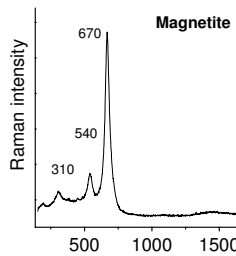


Cornell & Schwertmann. The Iron Oxides. Wiley-VCH Verlag (2003)

Iron oxide polymorphs (a selection)

Polymorph	Type	Symmetry	Spacegroup	Density/g cm ⁻³
Wustite, FeO		cubic	<i>Fm</i> 3 <i>m</i>	6
Magnetite, Fe ₃ O ₄	spinel	cubic	<i>Fd</i> 3 <i>m</i>	5.18
Hematite, α-Fe ₂ O ₃	corundum	trigonal	<i>R</i> 3 <i>c</i>	5.23
Maghemite, γ-Fe ₂ O ₃	spinel	cubic	<i>P</i> 4 ₃ 32	4.87
Goethite, α-FeOOH			2/ <i>m</i> 2/ <i>m</i> 2/ <i>m</i>	3.7
Lepidocrocite, γ-FeOOH			<i>Cmcm</i>	4

Each polymorph shows a characteristic Raman spectrum. . .



... but IR is more open to interpretation

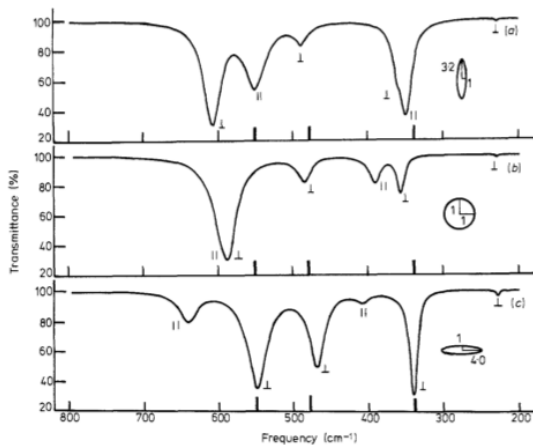


Figure 3. Calculated transmission spectra corresponding to three different particle shapes; (a) long prolate with $L_{\perp} = 0.45$ and $L_{\parallel} = 0.10$; (b) sphere with $L_{\perp} = L_{\parallel} = \frac{1}{2}$; (c) the flat oblate with $L_{\perp} = 0.15$ and $L_{\parallel} = 0.70$. Thick vertical bars on the abscissae indicate the observed peak frequencies.

Hematite IR/Raman peaks (literature)

TABLE 9: Calculated and Observed Wavenumbers for Hematite

obs ^{26,27} /cm ⁻¹	calcd/cm ⁻¹	sym species	activity	ions involved
225	228	A _{1g}	Raman	Fe,O
229	290	E _u	IR	Fe,O
247	200	E _g	Raman	Fe,O
293	294	E _g	Raman	Fe,O
299	327	E _g	Raman	Fe,O
310–335	310	E _u	IR	Fe,O
310–335	339	A _{2u}	IR	Fe,O
380–400	368	E _u	IR	Fe,O
380–400	378	A _{2u}	IR	Fe,O
412	391	E _g	Raman	Fe,O
440–470	454	E _u	IR	Fe,O
498	447	A _{1g}	Raman	Fe,O
613	466	E _g	Raman	Fe,O